Experimental Investigation and Statistical Modeling of FRP Confined RuC Using Response Surface Methodology

Xiong Feng [a], Rana Faisal Tufail [b*], Muhammad Zahid [c]

[a] Professor, College of Architecture and Environment, Sichuan University, Chengdu 610064, China.

[b] PhD Scholar, College of Architecture and Environment, Sichuan University, Chengdu 610064, China.

[c] PhD Scholar, University Teknology Petronas, Perak 32610, Malaysia.

Abstract

Scrap tires that are dumped to landfill is a serious problem in China and rest of the world. The use of rubber in concrete is an effective environmental approach to reduce the amount of scrap tires around the world. However, the loss in compressive strength of concrete is a major drawback of rubberized concrete. In this paper, the fiber reinforced polymer (FRP) confinement technique is used to overcome the drawbacks of rubberized concrete (RuC). A total of sixty six RuC cylinders were tested in axial compression. The cylinders were cast using recycled rubber to replace, a) 0-50 percent fine aggregate volume, b) 0-50 percent coarse aggregate volume, and c) 40-50 percent fine and coarse aggregate volume. Twenty seven cylinders of the latter mix were then confined with one, two and three layers of CFRP jackets. Concrete suffered a substantial reduction in compressive strength up to 80 percent by fine and coarse aggregate replacement with rubber content. However, CFRP jackets recovered and further enhanced the axial compressive strength of RuC up to 600% over unconfined RuC. SEM was performed to investigate the microstructural properties of RuC. Statistical models were developed on the basis of experimental tests for FRP confined RuC cylinders using response surface method. The effect of variable factors; unconfined concrete strength, rubber replacement type and number of FRP layers on confined compressive concrete strength was investigated. The regression analysis was performed to develop the response equations based on quadratic models. The predicted and experimental test results were found in good agreement as the variation between experimental and predicted values were less than 5%. Furthermore, the difference between predicted and adjusted R^2 was found to be less than 0.2 which shows the significance of the statistical models. These proposed statistical models can provide a better understanding to design the experiments and the parameters affecting FRP-confined RuC cylinders.

Keywords: FRP; Concrete; Cylinders; Response Surface Methodology; Rubberized Concrete.

1. Introduction

Scrap tire management has become a serious issue due to the increase in tire production. Worn out tires cause serious health and environmental issues. Scrap tires contain a high percentage of volcanized rubber which is difficult to recycle. Tires can also catch fire resulting in increased cost to extinguish it. Rubber content can be partially replaced by mineral aggregates in concrete, which is one of the possible recycling approaches. Several advantages of rubber have been reported in the literature [1]. High strength, flexibility and the ability to maintain its volume under compressive loading are some of the advantages of rubber. However, the addition of rubber can cause a significant loss in mechanical properties of concrete [1-5]. The reduction in compressive strength of rubberized concrete is a major drawback of using RuC in engineering practice [1]. A lot of studies have been conducted for partial replacement of mineral aggregate by

rubber content in concrete [1-10]. Low compressive and tensile strength as compared to normal concrete was reported by the addition of rubber particles in concrete [11, 12]. However, the amount of damage caused by the addition of rubber in compressive strength of rubberized concrete is dependent on the size, and type of rubber replacement [13]. A few inconsistent results for mechanical properties of RuC have been reported in the literature in terms of compressive strength, ductility and elastic modulus [11]. SEM results from previous literature show that RuC has high entrapped air content and weaker bonding as compared to the conventional concrete [14]. The high porosity of mix and weak bonding between concrete and rubber content results in reduced concrete compressive strength due to addition or replacement of rubber [15, 16]. A lot of researches have been conducted in recent years for fiber reinforced polymer (FRP) confinement of structures [17-22]. FRP jacketing of columns has become increasingly common in the construction industry. A lot of experimental studies have proven the effectiveness of FRP jackets for seismic resistance of conventional concrete columns due to its high strength and stiffness. Moreover, the jacketing of rubberized concrete (RuC) by FRP can recover the compressive strength loss due to rubber content. FRP jackets can significantly enhance the confined strength of FRP wrapped columns. [21, 22] The combination of rubberized concrete (RuC) and FRP jackets can result in a column with improved mechanical properties like strength and ductility.

Till date, a very few studies have been reported in the literature for FRP confinement of rubberized concrete. Li et al. conducted experiments on FRP wrapped rubberized concrete with 15 percent rubber replacement. Their results reported 23% strength enhancement for FRP confined RuC cylinders. Furthermore, axial strains of RuC cylinders with FRP jackets were recorded to be two times of normal concrete cylinders. It is worth to note that GFRP jackets were used in their research program [23]. Yousef et al performed an experimental study to increase the confined strength of RuC cylinders. CFRP cylinders cast in FRP tubes were used for confinement. High compressive strength up to 112.5 MPa was reported from their experimental study. However, stress-strain curves of CFRP wrapped rubberized concrete cylinders was almost similar to conventional concrete cylinders [22]. In an experimental study by Duarte et al., the ductility of the RuC samples confined by steel tubes was increased up to 50% but remained limited due to local bucking. [24]. Raffoul et al. investigated the effect of 2 and 3 aramid fiber reinforced polymer (AFRP) layers on mechanical properties for RuC containing 60% rubber content. Compressive strengths and axial strains up to 75 MPa and 5% were achieved [1]. A very few experimental studies exist in the literature for FRP confined RuC [1, 23]. However, according to the author's knowledge, no research has ever been conducted to investigate the behavior of CFRP confined RuC.

It is essential to utilize the robust tool for statistical modeling to better understand the behavior of FRP confined RuC. Response surface methodology (RSM) was used which is a powerful tool for analysis and design of experiments. Predictive models can be developed to compare the experimental data and predicted values. RSM technique uses a statistical method and develops a relationship between independent and dependent variables in the study [25]. RSM can be used with less effort and limited resources to analyze the experiments in a systematic method. The relationship between the independent input factors and dependent output variables can be drawn with the use of statistical models. Finally, a model can be developed to predict the output of experiments using dependent variables. It can indicate the sensitivity and effect of the independent input factors on the output factor [26]. The best possible solution from the 3D curves and statistical models can be developed. The advantages of RSM technique are, a) Limited number of experiments b) Relationship and regression models for input and output, c) Evaluation and development of statistical model with the desired output factor and input variables, d) Lesser time required for development of statistical models using RSM, and e) Validation of the predicted and experimental data. RSM technique is commonly used in the concrete industry but its use in FRP confined concrete is still novel. Several researchers have used this technique for modeling, optimization, and analysis for the experiments [25, 27].

This innovative research study aims to recover or even further enhance the loss in compressive strength of RuC by using CFRP jackets. The experimental results from this innovative research will contribute in the possible future use of FRP confined RuC for structural columns. Furthermore, the increased lateral dilation of RuC can be exploited by FRP jackets to develop a high strength and deformable concrete. The main objective of this paper is to investigate the CFRP confinement of RuC for the first time and apply the RSM technique to model the parametric factors affecting the FRP-confined RuC. The principal variables in this research study are number of FRP layers, unconfined concrete compressive strength, and type of aggregate replacement. The experimental results from FRP confined RuC tests are analyzed by RSM technique to form a predictive model based on dependent variables.

2. Experimental Program

This research study is comprised of 66 circular concrete cylinders. The program was divided into three groups having fine (0 to 50%), coarse (0 to 50%), fine and coarse mineral aggregate (40 to 50%) replacement by rubber content. The mechanical performance of rubberized concrete was investigated and the main parameters of the study were an unconfined concrete strength, the percentage of rubber content and number of fiber reinforced polymer (FRP) layers.

2.1. Materials

Portland Limestone Cement containing 10% limestone was used for all mixes according to ASTM C1157. Fly Ash (FA) and Silica Fume were used in this research to obtain the target strength. Locally available fine aggregate was used with a size and specif gravity of 0-5 mm and 2.65 respectively. Two sizes were selected for the coarse aggregates i.e.,

5-10 and 10-20 mm. Figure 1 represents the rubber and aggregate particle size used in this study. The rubber content was divided into two groups i.e., 0-5 and 5-20 mm for fine and coarse aggregate replacement respectively. The properties of aggregate and rubber content are shown in Table1.

Table 1. Physical properties of mineral aggregate and rubber

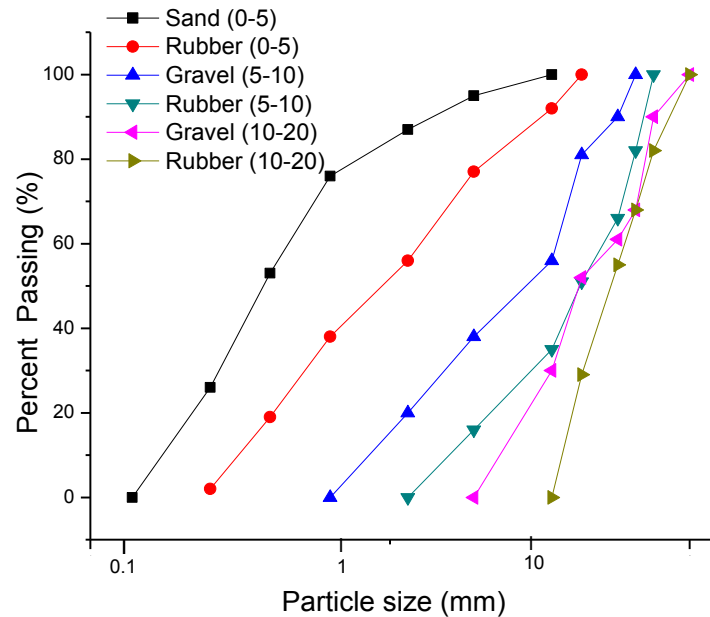| Material (size in mm)	Apparent density (g/cm^3)	Oven dry density (g/cm^3)	Water absorption (%)	Specific gravity	Bulk density (g/cm^3)	Flakiness Index
Rubber (0-5)	0.78	--	--	--	0.42	--
Rubber (5-10)	1.08-1.24	1.0-1.10	4.90-7.90	1.08	0.46	6.3-7.9
Rubber (10-20)	2.60	2.54	0.78-1.26	1.08	0.48	9.8-15.5
Sand (0-5)	2.60	2.54	0.5	1.08	1.74	--
Gravel (5-10)	2.67	2.56	1.22	2.60	1.48	6.80
Gravel (10-20)	2.67	2.56	1.22	2.60	1.54	9.70

Figure 1. Particle size distribution of mineral aggregates and rubber

2.2. Response Surface Method

Response surface method is a statistical method to develop a relationship between independent and dependent variables. Independent dependent variables are known as factors and response respectively. The method involves four different procedures to develop or validate a model as, a) Designing of the experiments using the RSM design tool, b) Experiments are performed to get response values for different variables, c) Development of a model with different response functions and variables, and d) Optimizing the proposed model using RSM techniques used in the software [28]. Various design models can be used like linear, quadratic or cubic to process the model. These models can be used to predict the response like the compressive strength of concrete. Models and approaches used for response surface method are shown in Figure 2 [29].
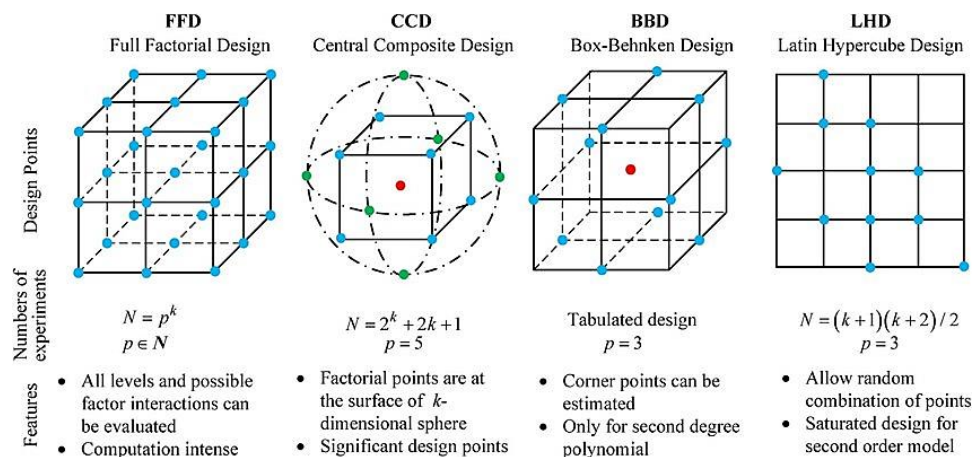

Figure 2. Models and approaches used for response surface method [29]

The quadratic model was used in this research study to predict the response for different variables like a number of FRP sheets, unconfined strength, and percentage of rubber content. Compressive strength was the response predicted by quadratic models. Unconfined strength and number of FRP jackets used to confine concrete columns significantly changes the response of concrete cylinders. The range of independent variables like unconfined strength and number of FRP layers was determined from the experimental test values. The commercial software (Design Expert) was used to design and analyze the experiments. The software uses the optimal quadratic model as shown in the Equation 1.

$$y = \beta_0 + \sum_{i=1}^{k} \beta_i x_i + \sum_{i=1}^{k} \beta_{ii} x_i^2 + \sum_{i,j} \beta_{ii} x_i x_j + \varepsilon \tag{1}$$

Where a predicted response is designated by y, xi and xj are the preparation variables. The numbers of factors to be optimized and random error are designated by k and ε respectively.

2.3. Casting Procedure

The concrete constituents were mixed as, 1) Rubber particles and mineral aggregates were mixed for 30 seconds. The rubber particles were used as received whereas; the mineral aggregates were saturated surface dry, 2) Water was mixed in two intervals, 3) The mix was allowed to rest for around 3 minutes, 4) The binder materials (Silica Fume, Fly Ash, and Cement) were added and then the remaining water was poured followed by the addition of admixtures in the mix, 5) The concrete was mixed for approximately three minutes. The cylinders were cast in two layers and vibrated using a vibration table for around 20 seconds per layer. Later, the specimens were covered with plastic sheets and were de-molded after 24 hours. The specimens were put for curing in curing bath tank for 28 days.

2.4. FRP Fabrication and Jacketing of Concrete Cylinders

2.4.1. Physical and Mechanical Properties of FRP

The physical and mechanical properties of unidirectional CFRP fabric and cured laminate sheets are shown in Table 2. The tensile strength and elastic modulus of unidirectional CFRP fabric were 4100, 231000 MPa respectively. Percentage elongation for CFRP fabric as provided by the manufacturer was 1.7%. The standard value of Tensile strength, Tensile Elastic Modulus, elongation, and density for cured laminate jackets were 894 MPa, 65402 MPa, 1.7% and 1.8 g/cc respectively. The surface of specimens was cleaned by brush to get rid of sand and other impurities.

Table 2. Physical and mechanical properties of unidirectional CFRP fabric and cured laminate sheets

Property	CFRP fabric test values	Cured laminate values
Primary fiber direction	unidirectional	--
Tensile strength (MPa)	4100	894
Tensile elastic modulus (MPa)	231000	65402
Elongation (%)	1.7	1.33
Primary fiber direction	unidirectional	--

2.4.2. FRP Jacketing and Testing Procedure

The concrete cylinders were wrapped with unidirectional CFRP jackets. The carbon fiber sheets were wrapped manually around the cylinders using the wet layup technique. An overlap of ¾ inches was provided according to American Concrete Institute (ACI 318-08) in order to avoid premature failure or de-bonding of FRP sheets. Figure 3 shows the fabrication of CFRP jackets. Dust particles were removed from the surface of cylinders and the surface was made smooth before the applying adhesive on the concrete cylinders. The normal brush was used to remove unwanted particles before the application of adhesive and FRP sheets. The adhesive consisted of two components namely "a" and "b". The components were mixed with the desired ratio as recommended by the manufacturer. The adhesive was hardened after approximately 5 hours as mentioned in the manufacturer data sheet. One, two and three layers of FRP were wrapped on the cylinders. The cylinders were tested under axial compression using a compression testing machine having a 3000 kN load capacity. The specimens were tested using the standard protocol described in ASTM C39 [30]. The cylinders were loaded till failure using 0.25 MPa/sec loading rate. Figure 4 shows the general test setup.

Figure 3. Fabrication of FRP jackets

Figure 4. General view of the test setup

3. Results and Discussion

3.1. Failure Modes

The failure modes for each specimen from Group 1 to 3 were observed. The control concrete specimens for each group failed suddenly in an explosive manner. Similar failure mode was observed for specimens with low rubber content (10 to 20% Fine or Coarse aggregate replacement). However, the specimens with more rubber content (30, 40 and 50% Fine or Coarse aggregate replacement) failed in a gradual manner. Fine micro-cracks were observed for these specimens. More bulging was observed with higher rubber content. This increase in bulging with higher rubber content can be attributed to increased lateral dilation produced by rubber. Gypsum capping was provided on top and bottom of each specimen to avoid premature and local failure of specimens. The specimen with FRP confinement failed suddenly in an explosive manner dominated by the rupture of FRP sheets from the center and bottom portion. The typical failure mode of the CFRP wrapped column is shown in Figure 5.

Figure 5. Typical failure mode of CFRP wrapped column

3.2. Microstructural Observations

Figure 6 shows the microstructure SEM images of different RuC concrete samples. The poor adhesion between rubber content and cement paste is clearly shown in scanning electron microscopy (SEM) images. The poor bonding is attributed to the presence of zinc stearate which results in the creation of soap like layer near rubber. This layer is responsible for repelling water from the rubber content. The surface of rubber content seems to be rough and surrounded by loose particles. This poor bond between rubber content and cement paste is responsible for the reduced compressive strength of concrete.

Rubber content or voids can be seen by dark features in SEM images. Light and intermediate grey color show mineral aggregate and hydrated cement part respectively. Un-hydrated cement particles are shown by bright scattered spots in SEM image. The images also reveal large gaps between cement paste and rubber content. These gaps can be attributed to, a) Poor bonding and limited cement hydration, b) Detachment of rubber during the preparation of the specimen. The gaps were found to be more in concrete having a high percentage of rubber content. Visible cracks between cement paste and aggregates can also be seen from SEM images. Interfacial Transition Zone (ITZ) portion is much thinner in RuC samples as compared to controlled samples without rubber content.
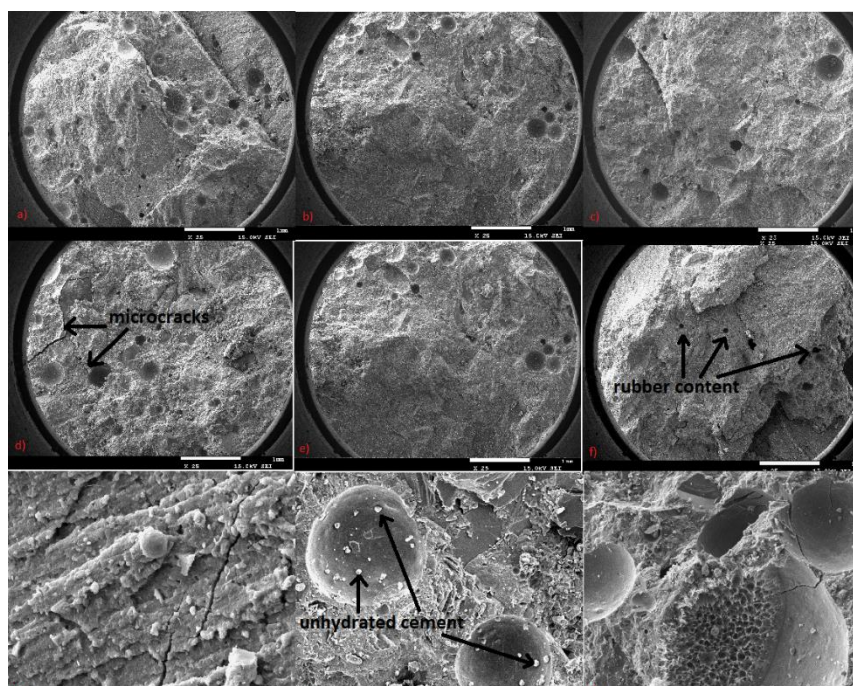

Figure 6. SEM images at 25x and 200x magnification

3.3. Effect of Rubber Replacement Type on Compressive Strength of Concrete

The addition of rubber in concrete resulted in reduced axial compressive strength of RuC as compared to conventional concrete. Table 3 shows the reduction in compressive strength of RuC for different mixes. The fine, coarse and combined fine and coarse aggregate replacement by rubber content is shown by C, F, and CF respectively. 14 to 55 percent reduction in compressive strength was observed for fine rubber replacement in RuC. The mix 50-F showed the highest reduction in compressive strength with 50% rubber content in group-1. It is worth to mention that the addition of rubber content in concrete leads to early cracking and premature crack formation. These factors lead to the loss of concrete strength and low ultimate axial compressive load capacity for concrete cylinders. Higher reduction in axial compressive strength was recorded in the mixes with coarse aggregate replacement as compared to the fine rubber replaced counterparts. A reduction of compressive strength up to 73 percent was recorded for coarse aggregate replacement in RuC (group-2). Highest percentage loss in compressive strength was observed for 50 percent rubber replacement in the mix (50-C). The strength loss in the range of 24 to 73 percent was observed for coarse aggregate replacement with rubber content in RuC. The decrease in compressive strength was more pronounced for coarse aggregate replacement by rubber content over the corresponding fine aggregate replaced RuC. Highest reduction in concrete compressive strength was observed for combined fine and coarse rubber replacement in RuC (group-3). The reduction in compressive strength up to 80% was recorded in this group i.e., higher than the group-1 and 2. Highest reduction in compressive strength was observed for the mix (50-CF), where the mineral aggregate in concrete was replaced with a combined 50% fine and coarse rubber content. Rubberized concrete shows higher lateral dilation than conventional concrete. The rubber particles also show higher lateral dilation when subjected to axial compressive loading. This phenomenon produces higher tensile stresses near rubber content in concrete. Furthermore, it is evident from the results that the addition of rubber particles in concrete cylinders results in a loss of axial compressive strength.

Figure 7 shows the predicted versus recorded test results for unconfined RuC (fine rubber replacement). The parametric variable factor for this statistical model was the percentage of rubber content. The output response parameter for this model was the percentage axial compressive strength loss in RuC. The predicted and recorded test values were in good agreement because the value of R^2 was less than 1. Normal probability plot for RuC (fine rubber replacement) is shown in Figure 8. Data is normally distributed because the data points are coincident with the straight line as shown in Figure 8. The regression equation "y=7.30+0.97×x" was developed to predict the compressive strength of RuC for fine rubber replacement. The parametric factor "x" and response "y" shows the percentage of rubber content and axial strength loss respectively. It is evident from the Figure 7 and 9 that the addition of rubber causes a reduction in compressive strength of concrete, where the predicted results are in close agreement with the experimental compressive strength results. The loss in strength of RuC cylinders is attributed to higher lateral dilation and premature crack formation in concrete as discussed earlier. Rubberized concrete showed higher lateral dilation than conventional concrete. These factors led to the loss of concrete strength and low ultimate axial compressive load capacity for concrete cylinders. Analysis of variance table (ANOVA) for the response is shown in Table 4. Figure 7 shows the experimental and predicted values for FRP confined RuC (coarse rubber replacement). Higher loss in axial compressive strength was observed for coarse rubber replacement in RuC as compared to fine rubber replacement. The predicted and test values were found to be in good agreement. Normal probability plot is shown in Figure 10 which shows that the straight 45-degree line and data points are nearly coincident. The regression equation "y=13.90 + 1.19×x" was developed for prediction of the unconfined axial strength of RuC for coarse rubber replacement. The parameters x and y shows the percentage of rubber content and axial compressive strength loss in RuC respectively. The statistical graph for RuC with both fine and coarse rubber replacement was not plotted. The reason was less number of parametric values for percentage rubber replacement in that group.

Table 3. Percentage reduction in compressive strength for RuC

Group-ID	Percentage rubber replacement (%)	Unconfined strength (fc') MPa	Percentage reduction in strength (%)
C	--	42	--
10-F	10	46	14
20-F	20	29	30
30-F	30	26	38
40-F	40	23	45
50-F	50	19	55
10-C	10	32	24
20-C	20	25	40
30-C	30	21	50
40-C	40	16	61
50-C	50	11	73
40-CF	40	11	73
50-CF	50	8	80

Table 4. Analysis of variance table (ANOVA) for the response

Standard order	Actual value	Predicted value	Residual	Leverage	Internally studentized residual	Influence on fitted value (IFV)
1	40	37.70	2.30	0.30	1.578	2.05
2	73	73.40	-0.40	0.60	-0.363	-0.371
3	61	61.50	-0.50	0.30	-0.343	-0.187
4	50	49.60	0.40	0.20	0.257	0.106
5	24	25.80	-1.80	0.60	-1.634	-4.98
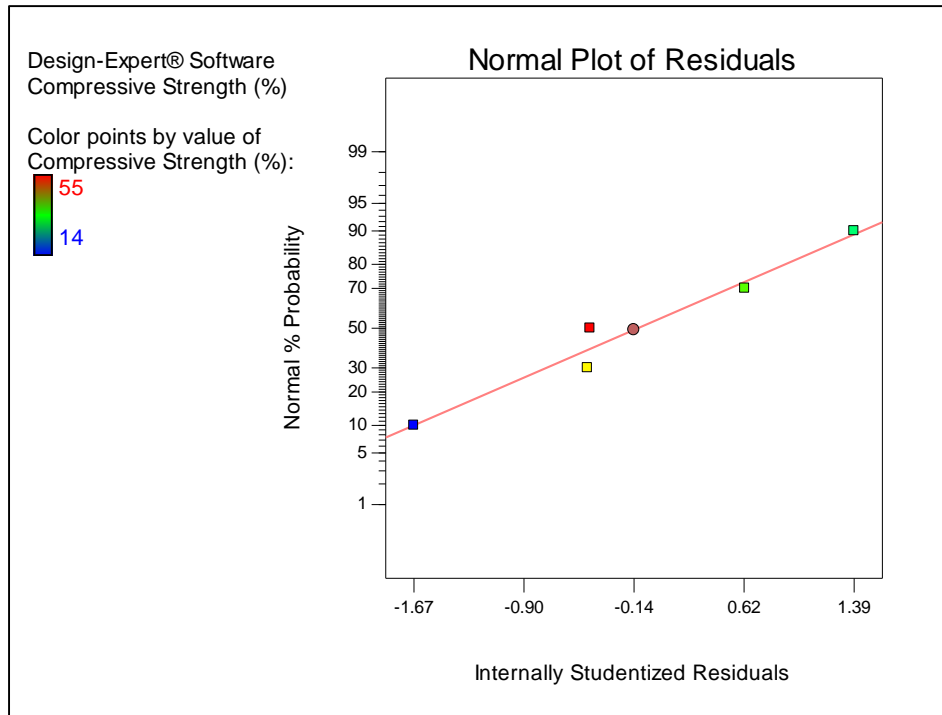
Figure 7. Predicted versus actual test results using RSM
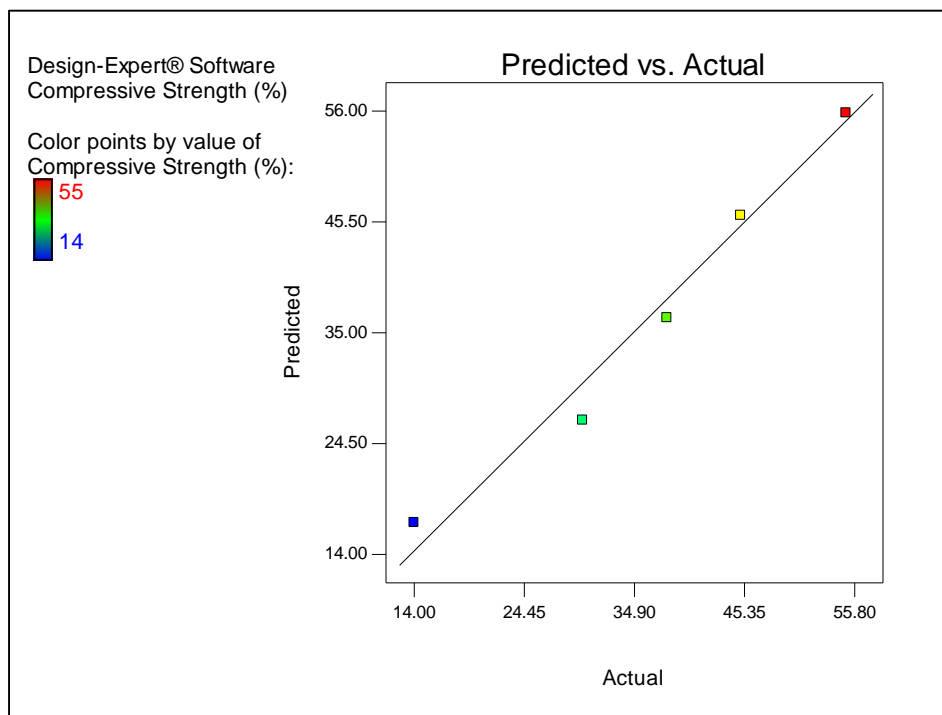
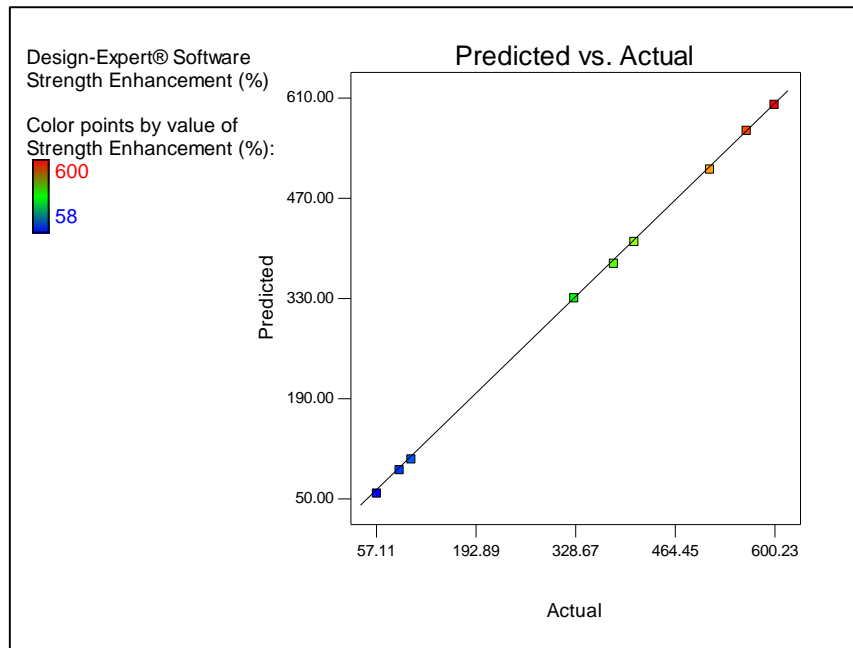
Figure 8. Normal plot of residuals using RSM technique

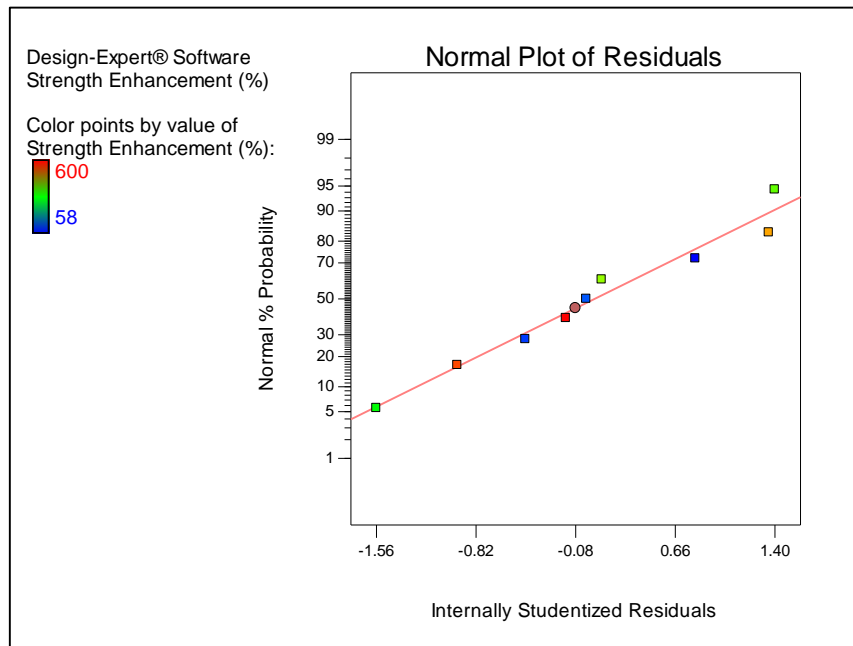**Figure 9. Predicted versus actual test results using RSM**

Figure 10. Normal plot of residuals using RSM technique

3.4. Effect of Unconfined Concrete Compressive Strength and Number of FRP Layers

In this section, the effect of fc' (unconfined compressive strength of concrete) and number of FRP layers on the compressive strength of FRP confined-RuC is investigated. Table.6 shows the unconfined compressive strength (fc'), confined compressive strength (fcc'), the confined ratio (experimental and theoretical) for FRP-confined RuC cylinders. The jacketing of rubberized concrete (RuC) by FRP recovered and further enhanced the compressive strength of rubberized concrete. 30 to 39 MPa confined compressive strength was recorded for CFRP confined RuC cylinders for 1 to 3 Layers of FRP sheets in group-1 respectively. The strength increment in FRP confined rubberized concrete strength was reported to be 105 percent of the unconfined RuC cylinders. A higher strength increment in the cylinders with coarse rubber replacement was reported. The test results indicated strength enhancement up to 409 percent for this group (group-2). Confined compressive strengths of 47 to 56 MPa were recorded for 1 to 3 layers of FRP jackets. This increment was higher than the group-1 with the same number of FRP jackets. Moreover, the highest increment in FRP confined RuC was recorded for combined fine and coarse rubber replacement in RuC. The confined compressive strength of 49 to 56 MPa was recorded for 1 to 3 layers of FRP jackets in this group. The test results indicated 500 percent increment for FRP confinement of rubberized concrete in group-3. The inclusion of rubber content in the concrete leads to increased lateral dilation of concrete. This lateral dilation of RuC activates the confining mechanism

of FRP jackets. It can be concluded that FRP jacketing can significantly increase the confined compressive strength of rubberized concrete over the unconfined concrete.

The RSM technique was employed to investigate the effect of parameters, a) Effect of unconfined axial compressive strength, and b) Number of FRP layers on strength enhancement for FRP confined RuC. It is evident from the results of the previous section that the addition of rubber content leads to a loss in concrete strength. However, FRP jackets successfully recovered and enhanced the compressive strength of rubberized concrete. The statistical parametric comparison for compressive strength enhancement ratios of FRP confined RuC cylinders are shown in Figure 11. The graphs were plotted using the response surface method (RSM). The contour plot, also known as the equipotential curve is very common in statistical modeling. The contour plot is a function of variables and the same value points that are connected along the curve [25]. The obtained model shows a reliable correlation between the response and parametric factors. The response factor for Figure 11 was the percentage enhancement ratio for FRP confined RuC cylinders. The parametric factors were the unconfined compressive strength of concrete and number of FRP layers. Based on the results from Figure 11 and 14, it can be concluded that the strength enhancement ratio is highly dependent on the unconfined concrete compressive strength. Analysis of variance table (ANOVA) for the response factor is shown in Table 5. Figure 14 depicts the perturbation curves to determine the sensitivity of the parametric factors. The parameter fc' (unconfined concrete compressive strength) shows a steep gradient in Figure 14 representing the sensitivity of this parametric factor. The parameter n (number of FRP layers) shows lesser steep slope as compared to fc', which in turn depicts lesser sensitivity of this factor. The graph for the response factor is also plotted in the form of 3D response surface as shown in Figure 12. Interaction plot shown in Figure 13 depicts how the factors collaborate for the output response. It is evident from the Figure 12 to 14 that strength enhancement of FRP confined RuC is more influenced by the factor fc'. The regression equation "$Y= 1109.20-102.6 \times fc'+95.9 \times n-1.93 \times fc'n+ 2.34(fc')^2-8.83n^2$" from the statistical model was developed. Strength enhancement percentage for FRP confined RuC cylinders is designated by the response factor Y. The parametric factors fc' and n shows the unconfined concrete compressive strength and number of FRP layers respectively.

It can be concluded from this section that carbon fiber reinforced polymer jackets are highly effective for the confinement of rubberized concrete. Furthermore, this increment in compressive strength is highly dependent on the unconfined concrete compressive strength.

Table 5. Analysis of variance table (ANOVA) for response surface quadratic model

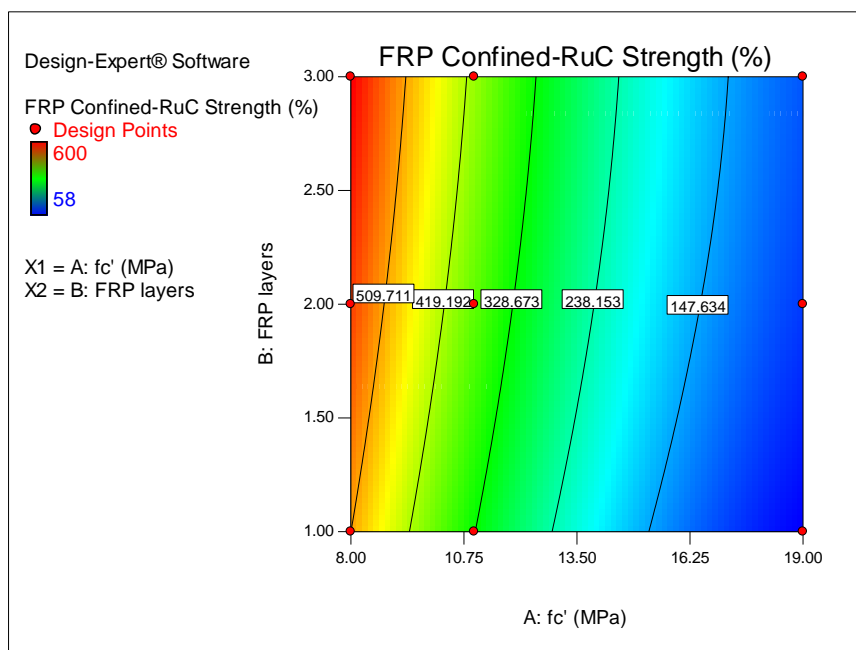| Source	Sum of Squares	df	Mean Square	F value	p-value, Prob > F
Model	3.508E+005	5	70154.08	7946.52	<0.0001
A-fc' (unconfined strength)	3.370E+005	1	3.370E+005	38174.39	<0.0001
B-n (number of FRP layers)	6941.88	1	6941.88	786.32	<0.0001
A2	5950.72	1	5950.72	674.05	0.0001
B2	156.06	1	156.06	17.68	0.0246
Residual	26.48	3	8.83	--	--

Figure 11. Contour plot for strength enhancement of FRP-confined RuC cylinders using response surface method
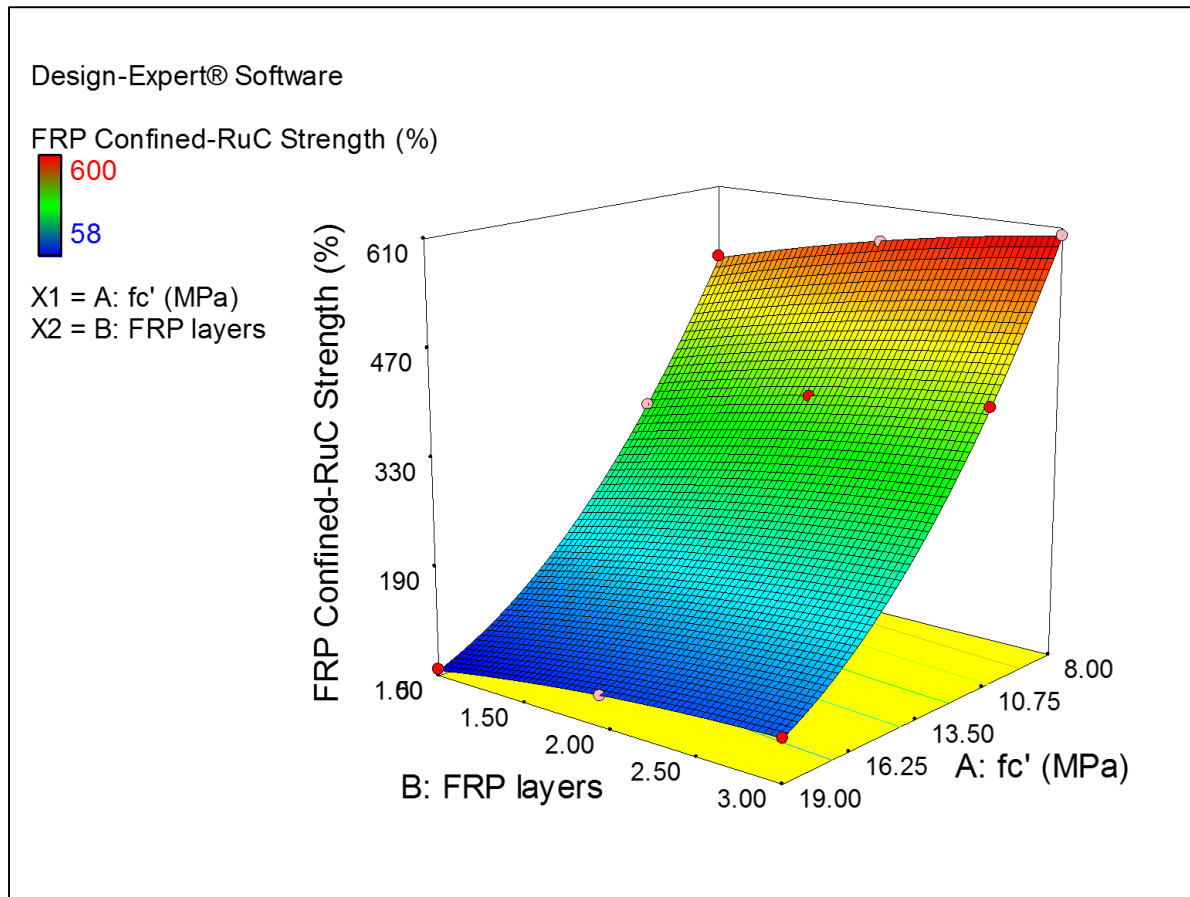
Figure 12. 3D response surface plot for strength enhancement of FRP-confined concrete cylinders using RSM
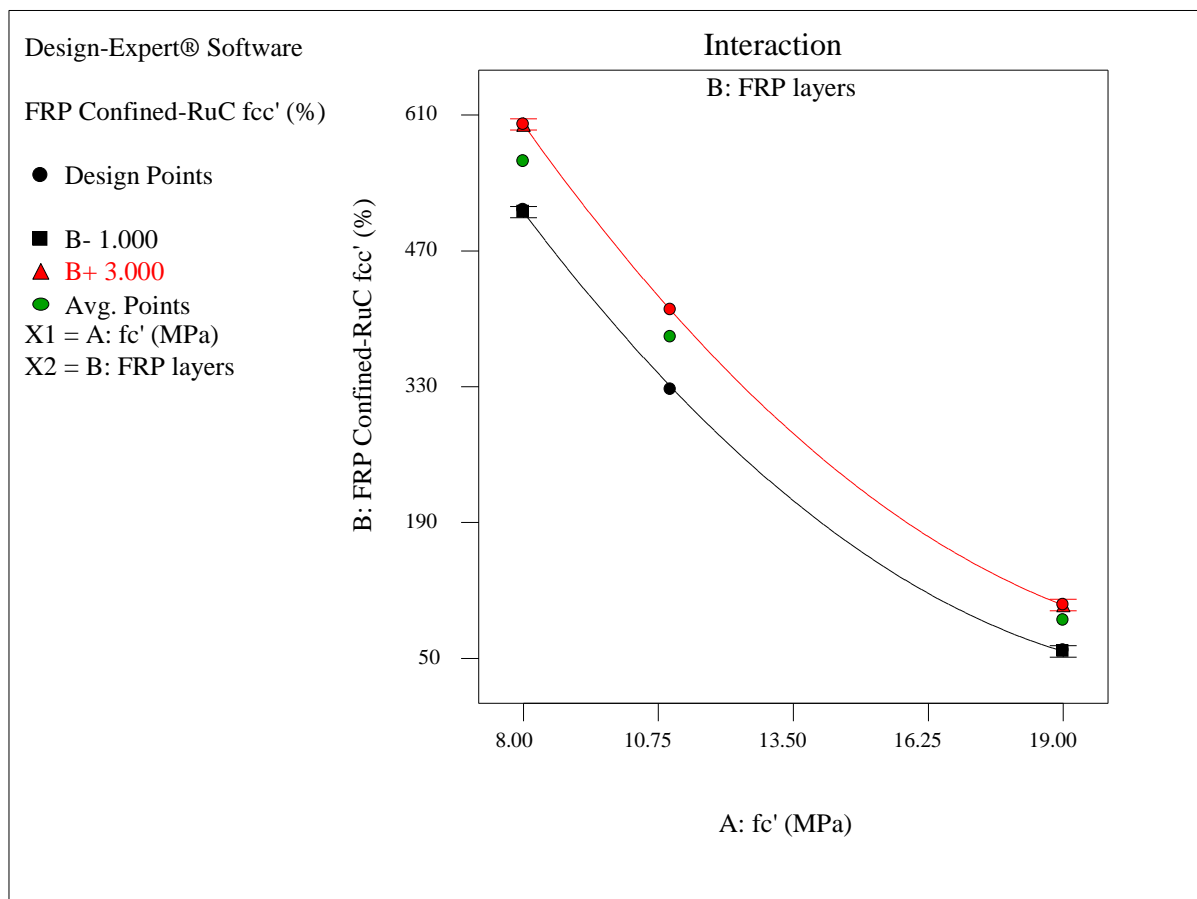

Figure 13. Interaction diagram for strength enhancement of FRP-confined concrete cylinders using RSM
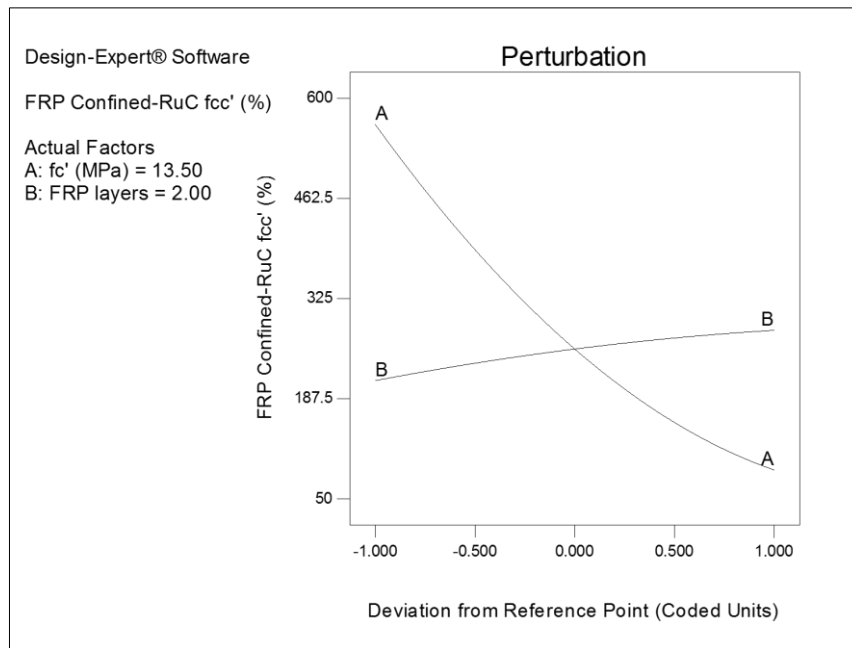
Figure 14. Perturbation plot for strength enhancement of FRP-confined concrete cylinders using response surface method

3.5. Design Guideline Predictions for FRP-Confined RuC

The experimental results of FRP confined RuC compressive strength are compared with the 3 North American design guidelines. North American design codes include American Concrete Institute (ACI 440.2R-2008), Canadian Standard Association (CSA-S806-02), and Intelligent Sensing for Innovative Structures Canada ISIS MO4 2001. Several design models and codes are available to predict the FRP confined strength of plain concrete. Stress-strain models have also been developed for FRP confined columns [31]. Most of the design models and equations have been developed from best fitting curves [32]. However, the behavior of RuC is very different as compared to the plain concrete. No design code is currently available to predict the strength of FRP confined RuC cylinders due to lack of data and experimental results. Majority of the confinement models and design codes are based on the Equation 2 [33].

$$f_{cc}' = f_{co}' + k_1 f_1'$$ (2)

Where fcc' and fco' is the confined and unconfined concrete strength respectively. Confinement pressure and lateral expansion coefficient are designated by k_1 and f_1 respectively. It is worth to note that the majority of the confinement model is based on normal strength plain concrete columns, the results may not be accurate for normal or high strength concrete confined by FRP. The approach and philosophy behind ACI code are based on the model presented by Mander et al. (1988) for steel confined concrete. The model was later modified by Spoelstra and Montri (1999) [34]. The model of Mander et al was adopted for FPR confined concrete strength enhancement. The philosophy behind using this model is that behavior of FRP and steel is same up to yield point i.e., linear elastic behavior. The fcc' provides the peak confined strength of concrete based on Mander curve but the confinement pressure is limited by ultimate FRP strain. The ultimate FRP strain is limited to lesser of 0.004 or 75 percent of ultimate FRP strain.

Table 6 shows the comparison of recorded experimental test results with the theoretical design guideline predictions for FRP confined RuC. The confinement equation for American Concrete Institute (ACI 440.2R-2008) design code to predict the confined strength and lateral confinement pressure is shown in Equation 3 [35].

$$f_{cc}' = f_{c}' + 3.3 k_a f_1$$ (3)

The confinement pressure f_1 depends on the unconfined concrete compressive strength, number of FRP layers, Elastic modulus of FRP, FRP effective strain and thickness of FRP layers. FRP effective strain is designated by εfe and depends on the coefficient kε. The load capacity equation for CSA-S806[36] is shown in the Equation 4.

$$f_{cc}' = 0.85 f_{c}' + k_1 k_s f_1$$ (4)

The response factor (fcc') depends on the unconfined concrete compressive strength and shape factor. The shape factor is considered to be equal to 1 for circular concrete cross-sections. The confinement pressure for Canadian Standard Association (CSA-S806-02) and American Concrete Institute (ACI 440.2R-2008) depends on the same parameters. Effective strain for CSA S-806 is the least value of 0.004 E_f and 0.75*ultimate FRP strain. American Concrete Institute (ACI 440.2R-2008) and Canadian Standard Association (CSA-S806-02) design code predicted reasonable axial strength

values of fiber reinforced rubberized concrete (FRuC) for 19 MPa unconfined compressive strength. High variation in theoretical and experimental compressive strength values was observed for 8 and 11 MPa unconfined strength. ISIS underestimate and overestimate the recorded test results for FRP confined RuC as shown in Table 6. Higher safety factors are considered by CSA, ISIS, fib and CS TR-55 design codes as compared to ACI. However, ACI and CSA apply reduction factors for materials and composition of FRP, the process of its manufacturing and exposure conditions for the structure.

The proposed equation based on the statistical modeling and regression analysis shows reasonable values for FRP confinement of rubberized concrete. The statistical model is significant as the proposed results are in good agreement with the recorded test values as shown in Table 6. The current international design guidelines developed for conventional concrete confinement does not account for increased lateral expansion by RuC. The philosophy behind the proposed equation is the early development of confinement pressure by FRP jackets for FRP confined RuC. Confinement factor was modified in-order to account for higher lateral dilation of RuC. This lateral dilation for RuC can be further exploited resulting in promising results for confinement. The proposed confinement equation for RuC is shown in the Equation 5.

$$f_{cc'} = P[f_{c'} + 3.3k_a f_1] \tag{5}$$

Where as:

P is the lateral dilation coefficient ranging from 1.08 to 2.1. Confinement pressure f_1 is shown in Equation 6.

$$f_1 = \frac{2E_f nt\varepsilon_{fr}}{D} \tag{6}$$

Where E_f= tensile elastic modulus of FRP, n= number of FRP layers, t= thickness of FRP layer, ε_{fr}= ultimate tensile strain of FRP and D= diameter of the section.

Table 6. Experimental results versus theoretical design code predictions for FRP confined RuC

Group	Design Code	fc'	fcc'exp (MPa)	fcc'exp /fc'	fcc'theo (MPa)	fcc'theo/fc'	fcc'exp/ fcc'theo
1		19	30	1.578947	27	1.421053	1.111111
		19	36	1.894737	34	1.789474	1.058824
		19	39	2.052632	43	2.263158	0.906977
2	ACI 440.2R-2008	11	47	4.272727	19	1.727273	2.473684
		11	52	4.727273	27	2.454545	1.925926
		11	56	5.090909	33	3	1.69697
3		8	49	6.125	16	2	3.0625
		8	53	6.625	24	3	2.208333
		8	56	7	31	3.875	1.806452
1		19	30	1.578947	25	1.315789	1.2
		19	36	1.894737	33	1.736842	1.090909
		19	39	2.052632	41	2.157895	0.95122
2	CSA-S806-02	11	47	4.272727	18	1.636364	2.611111
		11	52	4.727273	26	2.363636	2
		11	56	5.090909	34	3.090909	1.647059
3		8	49	6.125	15	1.875	3.266667
		8	53	6.625	23	2.875	2.304348
		8	56	7	32	4	1.75
1		19	30	1.578947	30	1.578947	1
		19	36	1.894737	48	2.526316	0.75
		19	39	2.052632	67	3.526316	0.58209
2	ISIS MO4 2001	11	47	4.272727	17	1.545455	2.764706
		11	52	4.727273	28	2.545455	1.857143
		11	56	5.090909	39	3.545455	1.435897
3		8	49	6.125	13	1.625	3.769231
		8	53	6.625	21	2.625	2.52381
		8	56	7	29	3.625	1.931034

		19	30	1.578947	29	1.034483	1.034483
1		19	36	1.894737	35	1.028571	1.028571
		19	39	2.052632	37	1.054054	1.054054
		11	47	4.272727	46	1.021739	1.021739
2	Proposed Equation	11	52	4.727273	51	1.019608	1.019608
		11	56	5.090909	56	1	1
		8	49	6.125	48	1.020833	1.020833
3		8	53	6.625	53	1	1
		8	56	7	57	0.982456	0.982456

3.6. Validation of Statistical Models (ANOVA)

Analysis of variance (ANOVA) table is shown in Table 7. The ANOVA models were statistically validated as the predicted and adjusted values of R^2 for the models are less than 0.2. The predicted and test values are in good agreement as shown in Table 5 and 7. Moreover, the adequate precision of the response factor in the statistical models was more than 4 which shows the acceptance and satisfactory performance of these models. The significance of the model can be predicted from the higher magnitude of F value and lower values for probability. Probability values less than 0.005 depicts the satisfactory performance of the statistical and regression models. [25, 37] The probability values are lesser than 0.005 for the parametric factors used in this research as shown in Table.7. Table.7 shows the statistical model validation factors obtained from analysis of variance (ANOVA).

Table 7. Statistical model validation for response factors

Response	Percentage compressive strength loss in RuC	Strength enhancement ratio	Compressive strength of concrete (MPa)
Standard Deviation	2.47	1.67	1.45
R-squared	0.9871	0.9961	0.8893
Adjusted R-squared	0.9747	0.9921	0.8677
Predicted R-squared	0.7821	0.9980	0.8683

4. Conclusions

This paper utilizes the RSM technique to develop the statistical models using parametric factors affecting the performance of FRP-confined RuC. The principal variables in this research study were number of FRP layers, unconfined concrete compressive strength, and type of aggregate replacement. Based on the results of this study, the following conclusions can be drawn:

- Significant reduction in compressive strength of RuC was observed for a higher percentage of rubber content replacement in the concrete mix. Furthermore, a higher reduction in axial compressive strength up to 80% was recorded for 50% rubber replacement in RuC. The developed regression equations could predict the reduction in compressive strength of RuC with accuracy as the RSM models were statistically validated.

- CFRP jackets can recover and further enhance the compressive strength of RuC. Strength enhancement up to 105, 409 and 600 percent was recorded for 3L CFRP confined RuC over unconfined RuC in group 1, 2 and 3 respectively.

- The strength enhancement for FRP confined RuC is highly dependent on the unconfined concrete compressive strength. Analysis of variance (ANOVA) and perturbation curves shows the higher sensitivity of the parametric factor (fc') which depicts the higher influence of this parameter on the performance of FRP confined RuC.

- The principal parametric factor n (number of FRP layers) fewer influences the strength enhancement provided by CFRP jackets for FRP confined RuC.

- Response surface method can be used to design or analyze the experiments. It is worth to highlight that RSM technique can predict the response for any variable factors involved in strength enhancement of FRP confined RuC. Unconfined concrete compressive strength, rubber replacement type and the number of FRP layers were used as the parametric factors in this study.

- American Concrete Institute (ACI 440.2R-2008) and Canadian Standard Association (CSA-S806-02) design code predicted reasonable axial strength values of FRP confined RuC for 19 MPa unconfined compressive strength. High variation in theoretical and experimental compressive strength values was observed for 8 and 11 MPa unconfined strength. ISIS underestimate and overestimate the recorded test results for FRP confined RuC.

- The proposed equation based on the statistical modeling and regression analysis shows reasonable values for FRP confinement of rubberized concrete. The statistical model was significant as the proposed results were in good agreement with the recorded test values.

- The robust tool for RSM technique reduces the time to design and analyze the experiments. Moreover, it improves the reliability and performance of the product.

5. Funding

6. Acknowledgments

7. Conflicts of Interest

The authors declare no conflict of interest.

8. References

[1] Raffoul, Samar, Reyes Garcia, David Escolano-Margarit, Maurizio Guadagnini, Iman Hajirasouliha, and Kypros Pilakoutas. "Behaviour of Unconfined and FRP-Confined Rubberised Concrete in Axial Compression." Construction and Building Materials 147 (August 2017): 388–397. doi:10.1016/j.conbuildmat.2017.04.175.

[2] Thomas, B.S. and R.C. Gupta, A comprehensive review on the applications of waste tire rubber in cement concrete. Renewable and Sustainable Energy Reviews, 2016. 54: p. 1323-1333. doi:10.1016/j.rser.2015.10.092.

[3] Sengul, O., Mechanical behavior of concretes containing waste steel fibers recovered from scrap tires. Construction and Building Materials, 2016. 122: p. 649-658. doi:10.1016/j.conbuildmat.2016.06.113.

[4] Huang, Shan-Shan, Harris Angelakopoulos, Kypros Pilakoutas, and Ian Burgess. "Reused Tyre Polymer Fibre For Fire-Spalling Mitigation." Applications of Structural Fire Engineering (January 18, 2016). doi:10.14311/asfe.2015.056.

[5] Goulias, D.G. and A.-H. Ali, Evaluation of rubber-filled concrete and correlation between destructive and nondestructive testing results. cement, concrete and aggregates, 1998. 20(1): p. 140-144. doi:10.1520/cca10447j.

[6] Son, K.S., I. Hajirasouliha, and K. Pilakoutas, Strength and deformability of waste tyre rubber-filled reinforced concrete columns. Construction and building materials, 2011. 25(1): p. 218-226. doi:10.1016/j.conbuildmat.2010.06.035.

[7] Liu, Feng, Liang-yu Meng, Guo-Fang Ning, and Li-Juan Li. "Fatigue Performance of Rubber-Modified Recycled Aggregate Concrete (RRAC) for Pavement." Construction and Building Materials 95 (October 2015): 207–217. doi:10.1016/j.conbuildmat.2015.07.042.

[8] Xue, James, and Masanobu Shinozuka. "Rubberized Concrete: A Green Structural Material with Enhanced Energy-Dissipation Capability." Construction and Building Materials 42 (May 2013): 196–204. doi:10.1016/j.conbuildmat.2013.01.005.

[9] Najim, K.B. and M.R. Hall, Mechanical and dynamic properties of self-compacting crumb rubber modified concrete. Construction and building materials, 2012. 27(1): p. 521-530. doi:10.1016/j.conbuildmat.2011.07.013.

[10] Batayneh, M.K., I. Marie, and I. Asi, Promoting the use of crumb rubber concrete in developing countries. Waste management, 2008. 28(11): p. 2171-2176. doi:10.1016/j.wasman.2007.09.035.

[11] Youssf, O., R. Hassanli, and J.E. Mills, Mechanical performance of FRP-confined and unconfined crumb rubber concrete containing high rubber content. Journal of Building Engineering, 2017. 11: p. 115-126. doi:10.1016/j.jobe.2017.04.011.

[12] Youssf, O., M.A. ElGawady, and J.E. Mills. Experimental investigation of crumb rubber concrete columns under seismic loading. in Structures. 2015. Elsevier. doi:10.1016/j.istruc.2015.02.005.

[13] Youssf, O., J.E. Mills, and R. Hassanli, Assessment of the mechanical performance of crumb rubber concrete. Construction and Building Materials, 2016. 125: p. 175-183doi:10.1016/j.conbuildmat.2016.08.040.

[14] Hernández-Olivares, F., G. Barluenga, M. Bollati, and B. Witoszek. "Static and Dynamic Behaviour of Recycled Tyre Rubber-Filled Concrete." Cement and Concrete Research 32, no. 10 (October 2002): 1587–1596. doi:10.1016/s0008-8846(02)00833-5.

[15] Richardson, A.E., K.A. Coventry, and G. Ward, Freeze/thaw protection of concrete with optimum rubber crumb content. Journal of Cleaner Production, 2012. 23(1): p. 96-103. doi:10.1016/j.jclepro.2011.10.013.

[16] Sukontasukkul, P., Use of crumb rubber to improve thermal and sound properties of pre-cast concrete panel. Construction and Building Materials, 2009. 23(2): p. 1084-1092. doi:10.1016/j.conbuildmat.2008.05.021.

[17] Ozbakkaloglu, T. and Y. Idris, Seismic behavior of FRP-high-strength concrete–steel double-skin tubular columns. Journal of Structural Engineering, 2014. 140(6): p. 04014019. doi:10.1061/(asce)st.1943-541x.0000981.

[18] Youssf, O., M.A. ElGawady, and J.E. Mills, Displacement and plastic hinge length of FRP-confined circular reinforced concrete columns. Engineering Structures, 2015. 101: p. 465-476. doi:10.1016/j.engstruct.2015.07.026.

[19] Youssf, Osama, Mohamed A. ElGawady, and Julie E. Mills. "Static Cyclic Behaviour of FRP-Confined Crumb Rubber Concrete Columns." Engineering Structures 113 (April 2016): 371–387. doi:10.1016/j.engstruct.2016.01.033.

[20] Youssf, Osama, Mohamed A. ElGawady, Julie E. Mills, and Xing Ma. "Finite Element Modelling and Dilation of FRP-Confined Concrete Columns." Engineering Structures 79 (November 2014): 70–85. doi:10.1016/j.engstruct.2014.07.045.

[21] Liu, J. and S.A. Sheikh, Fiber-Reinforced Polymer-Confined Circular Columns under Simulated Seismic Loads. ACI structural journal, 2013. 110(6). doi:10.14359/51686150.

[22] Hassanli, R., O. Youssf, and J.E. Mills, Seismic performance of precast posttensioned segmental FRP-confined and unconfined crumb rubber concrete columns. Journal of Composites for Construction, 2017. 21(4): p. 04017006. doi:10.1061/(asce)cc.1943-5614.0000789doi:10.1061/(asce)cc.1943-5614.0000789.

[23] Li, G., S.-S. Pang, and S.I. Ibekwe, FRP tube encased rubberized concrete cylinders. Materials and structures, 2011. 44(1): p. 233-243. doi:10.1617/s11527-010-9622-8.

[24] Duarte, A.P.C., B.A. Silva, N. Silvestre, J. de Brito, E. Júlio, and J.M. Castro. "Tests and Design of Short Steel Tubes Filled with Rubberised Concrete." Engineering Structures 112 (April 2016): 274–286. doi:10.1016/j.engstruct.2016.01.018.

[25] Zahid, Muhammad, Nasir Shafiq, M. Hasnain Isa, and Lluis Gil. "Statistical Modeling and Mix Design Optimization of Fly Ash Based Engineered Geopolymer Composite Using Response Surface Methodology." Journal of Cleaner Production 194 (September 2018): 483–498. doi:10.1016/j.jclepro.2018.05.158.

[26] Anderson, M. and P. Whitcomb, Find the optimal formulation for mixtures. Stat-Ease Inc, Minneapolis, 2002. doi:10.2307/2347648.

[27] Zahid, M., N. Shafiq, and A. Jalal, Investigating the effects of solarcure curing method on the compressive strength, microstructure and polymeric reaction of fly ash based geopolymer. Construction and Building Materials, 2018. 181: p. 227-237. doi:10.1016/j.conbuildmat.2018.06.046.

[28] Son, Donghee, Jongha Lee, Shutao Qiao, Roozbeh Ghaffari, Jaemin Kim, Ji Eun Lee, Changyeong Song, et al. "Multifunctional Wearable Devices for Diagnosis and Therapy of Movement Disorders." Nature Nanotechnology 9, no. 5 (March 30, 2014): 397–404. doi:10.1038/nnano.2014.38.

[29] Lian, B., T. Sun, and Y. Song, Parameter sensitivity analysis of a 5-DoF parallel manipulator. Robotics and Computer-Integrated Manufacturing, 2017. 46: p. 1-14. doi:10.1016/j.rcim.2016.11.001.

[30] Standard, A., Standard Test Methods for Compressive Strength of Cylindrical Concrete Specimens. ASTM C39, 2010. doi:10.1201/9781420091175-c18.

[31] Lam, L. and J. Teng, Design-oriented stress–strain model for FRP-confined concrete. Construction and building materials, 2003. 17(6-7): p. 471-489. doi:10.1016/s0950-0618(03)00045-x.

[32] Fardis, M.N. and H. Khalili. "Concrete Encased in Fiberglass-Reinforced Plastic." ACI Journal Proceedings 78, no. 6 (1981). doi:10.14359/10527.

[33] Pessiki, Stephen, Kent A. Harries, Justin T. Kestner, Richard Sause, and James M. Ricles. "Axial Behavior of Reinforced Concrete Columns Confined with FRP Jackets." Journal of Composites for Construction 5, no. 4 (November 2001): 237–245. doi:10.1061/(asce)1090-0268(2001)5:4(237).

[34] Spoelstra, Marijn R., and Giorgio Monti. "FRP-Confined Concrete Model." Journal of Composites for Construction 3, no. 3 (August 1999): 143–150. doi:10.1061/(asce)1090-0268(1999)3:3(143).

[35] Yazici, Veysel, and Muhammad N. S. Hadi. "Normalized Confinement Stiffness Approach for Modeling FRP-Confined Concrete." Journal of Composites for Construction 16, no. 5 (October 2012): 520–528. doi:10.1061/(asce)cc.1943-5614.0000283.

[36] Bisby, L.A., A.J. Dent, and M.F. Green, "Comparison of Confinement Models for Fiber-Reinforced Polymer-Wrapped Concrete." ACI Structural Journal 102, no. 1 (2005). doi:10.14359/13531.

[37] Subasi, Abdussamet, Bayram Sahin, and Irfan Kaymaz. "Multi-Objective Optimization of a Honeycomb Heat Sink Using Response Surface Method." International Journal of Heat and Mass Transfer 101 (October 2016): 295–302. doi:10.1016/j.ijheatmasstransfer.2016.05.012.